

Short Communication

Electrochemical Corrosion Behavior of the Copper Current Collector in the Electrolyte of Lithium-ion Batteries

Shuowei Dai^{1,2}, Jian Chen^{1,2}, Yanjie Ren^{1,2,*}, Zhimin Liu^{1,2}, Jianlin Chen^{1,2},
Cong Li^{1,2}, Xinyuan Zhang^{1,2}, Xiao Zhang^{1,2} and Taofang Zeng^{1,2}

¹ School of Energy and Power Engineering, Changsha University of Science & Technology, Changsha, Hunan 410014, China

² Key Laboratory of Energy Efficiency and Clean Utilization, Education Department of Hunan Province, Changsha University of Science & Technology, Changsha, Hunan 410014, China

*E-mail: yjren1008@163.com

Received: 24 July 2017 / Accepted: 3 September 2017 / Published: 12 October 2017

Copper is usually used as an anode current collector in lithium-ion batteries. Its stability in the organic electrolyte impacts the performance of the lithium-ion battery. In this paper, the corrosion mechanism of the copper current collector in the electrolyte of lithium-ion batteries was examined by electrochemical impedance spectroscopy (EIS) and polarization measurements. The microstructures of copper were observed by scanning electron microscopy (SEM) and energy dispersive spectroscopy (EDS). The fitted results of electrochemical impedance spectroscopy showed that R_f and R_t increased at the initial stage of exposure to the electrolyte indicating that a protective layer formed. After exposure to the electrolyte for up to 720 h, pitting holes could be clearly observed on the surface of copper.

Keywords: Lithium-ion Batteries, Copper current collector, Electrochemical impedance spectra, Corrosion mechanism

1. INTRODUCTION

Lithium-ion batteries have been widely used in mobile phones and other portable electronic devices as a clean and efficient secondary battery because of their high volume and energy densities in comparison with other rechargeable batteries. The stability of active materials in the battery is crucial to the maintenance of high power and energy density of lithium-ion batteries. [1-3] To date, a variety of anodic and cathodic materials, such as LiMn_2O_4 , Co_3O_4 , etc, have been studied under different conditions. [4-6] Current collectors are important components of lithium ions batteries that load the

active substance, collect current, minimize the internal resistance and enhance cycling stability. [7] However, current collectors usually suffer from severe corrosion damage in the electrolyte of lithium-ion batteries. Unfortunately, the corrosion products on the current collectors separate electrode materials and current collectors, further impacting the performance of lithium-ion batteries.

Previous studies focused primarily on the corrosion behavior of aluminum current collectors in lithium-ion batteries. Zhang et al observed that aluminum current collectors are susceptible to localized corrosion in battery electrolytes containing LiPF_6 . [8] Hyams et al compared the corrosion resistance of aluminum current collectors in high-power lithium-ion batteries with cycling at 25°C and 45°C. The results showed that there is an increase in percentage of pit area, the number of pits, pit size distribution and pit depth at 45°C. [9] Kramer et al. proposed that carbonates and particular lactones can cause intense corrosion of the aluminum collector in lithium-ion batteries, but adiponitrile results in insignificant corrosion when used as a pure solvent. [10] Streipert argued that the formation of a passivation films on aluminum and the decomposition of LiPF_6 are ongoing processes, which permit the dissolution phenomenon to occur in long-term applications. [11]

As a negative current collector, copper is also subjected to a continuous corrosion in the organic conductive solution because of the residual water. Recent research on the degradation of the copper current collector was devoted primarily to its corrosion products and variations in properties resulting from the decomposition of electrolytes. Shu et al revealed the possible corrosion products of copper in the electrolyte of a lithium-ion battery and considered that the existence of HF destroys the oxide film of inorganic compounds such as copper oxides. [12] Peng suggested that the reduction of the electrolytes provided limited protection for the Cu foil in ethylene carbonate (EC)/ dimethyl carbonate (DMC) solutions. [13]

However, until now, there is little information available about the corrosion mechanism of copper in the electrolyte of lithium-ion batteries. With an aim to obtain more information about the degradation of copper, the corrosion performance of copper in the electrolyte of lithium-ion batteries was investigated by electrochemical methods in the present study.

2. EXPERIMENTAL PROCEDURES

2.1 Sample preparation

Strips (5 mm x 5 mm x 10 mm) of copper (99.95%, commercial T1 pure copper) were polished and cleaned with acetone, followed by dry-air blowing to remove the solvent residue and dirt. All electrochemical measurements were carried out at ambient temperature in an electrolyte containing 1 M LiPF_6 in a mixture of ethylene carbonate (EC), methyl ethyl carbonate (EMC) and dimethyl carbonate (DMC) (1:1:1, V/V/V). The containers were sealed to avoid the ingress of oxygen.

2.2 Electrochemical measurements

A conventional three-electrode system was used for the electrochemical measurements, with a copper sheet as the counter-electrode and a silver sheet as the reference electrode. The corrosion tests

of the coated samples with a working surface area of 0.5 cm^2 were conducted with a Zahner (Zennum) potentiostat/galvanostat in the electrolyte at room temperature. Potentiodynamic polarization was undertaken with a potential scanning rate of 60 mV min^{-1} . Electrochemical impedance measurements were conducted in the range of 0.01 Hz – 100 kHz , with an amplitude of 10 mV for the input sine wave voltage.

2.3 Microstructure characterization

The corroded specimens were cleaned with deionized water and dried after corrosion testing. The microstructure of the samples before and after the immersion test was examined by a JSM-6360LV scanning electron microscopy (SEM) system. The analysis of elemental compositions was examined by energy dispersive spectroscopy (EDS).

3. RESULTS AND DISCUSSION

3.1 Surface morphology

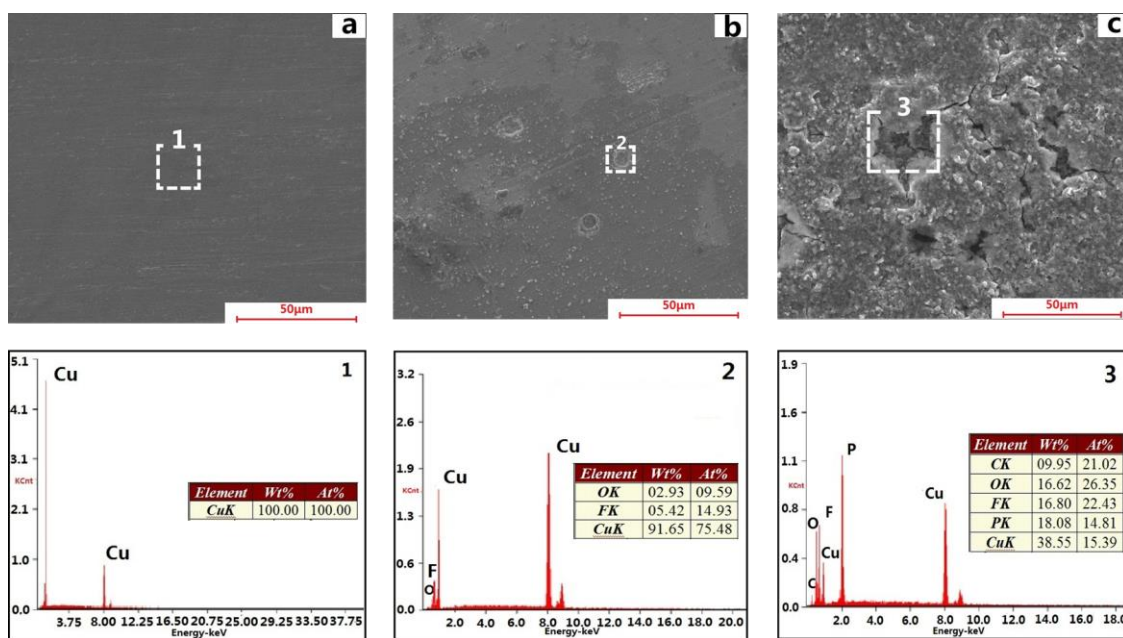


Figure 1. Surface morphology of copper at different stages with EDS analysis: (a) before the immersion test, (b) immersed for 480 h in the electrolyte, and (c) immersed for 720 h in the electrolyte

The surface morphologies and the corresponding EDS spectra of as-received and corroded copper in the electrolyte are shown in Figure 1. The surface of the pristine specimen is smooth and undisturbed (as shown in Figure 1a). However, clear holes with a diameter of approximately $10 \mu\text{m}$ can be observed on the surface of copper immersed for 480 h, indicating that the copper sustains

pitting corrosion in the electrolyte(as shown in Figure 1b). After immersion for 720 h, a corrosion product layer with enlarged pitting holes and micro-cracks can be observed. The pitting holes exhibit a certain depth. EDS results reveal that only Cu is detected for as-received copper. In the case of the specimen exposed to the electrolyte for 480 h, Cu, F and O elements are found in the holes, indicating that the corrosion products are composed of copper fluorides and copper oxides. For the specimen immersed for 720 h, Cu, C, O, F and P are detected in the holes, as also reported by Shu et al. [12] In comparison, the elemental concentrations (except for Cu) of the latter are higher than the former. The existence of F or P also proves that LiPF_6 in the electrolyte has a pronounced influence on the corrosion damage of copper current collectors. Zhao et al argued that the trace amount of water in the electrolyte reacts with the decomposition products of LiPF_6 and produces HF, which is aggressive towards the copper current collector. [14] The underlying corrosion mechanism is elaborated in a latter section.

3.2 Corrosion behavior of copper in the electrolyte

3.2.1 Potentiodynamic polarization curves

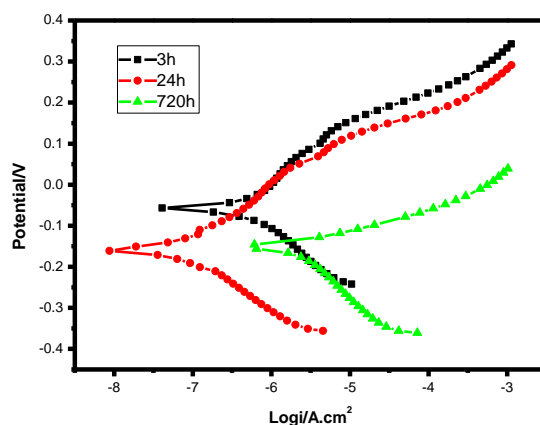


Figure 2. Potentiodynamic curves of copper in the electrolyte after immersion for 3 h, 24 h and 720 h (scanning rate: 1 mV/s)

Table 1. Electrochemical parameters of the potentiodynamic curves of copper in the electrolyte

Time(h)	E_{corr} (V)	I_{corr} ($\mu\text{A}\cdot\text{cm}^{-2}$)	β_a (V/Dec)	β_c (V/Dec)	R_p (Ωcm^{-2})
3	-0.054	0.416	0.195	0.171	9.423E4
24	-0.161	0.047	0.159	0.127	6.523E5
720	-0.152	2.081	0.062	0.179	9.388E3

Figure 2 shows the potentiodynamic polarization curves for copper after immersion for 3 h, 24 h and 720 h in the electrolyte. It can be observed that active dissolution occurs on the copper at free

corrosion potential in all cases. The corrosion potential moves towards the cathodic direction after immersion for 24 h and 720 h compared with that exposed to the electrolyte for 3 h. Electrochemical parameters namely, corrosion potential (E_{corr}), corrosion current density (I_{corr}), and cathodic and anodic Tafel slopes (β_c and β_a) were calculated from the Tafel extrapolation of the polarization plots. The polarization resistance of R_p are determined by the equation as follows: [15]

$$R_p = \frac{\beta_a \beta_c}{2.3 I_{corr} (\beta_a + \beta_c)} \quad (1)$$

All parameters are listed in Table 1. The corrosion current densities of specimens corroded for 3 h, 24 h and 720 h are $0.416 \mu\text{A}\cdot\text{cm}^{-2}$, $0.047 \mu\text{A}\cdot\text{cm}^{-2}$ and $2.081 \mu\text{A}\cdot\text{cm}^{-2}$, respectively. Compared with the specimen corroded for 3 h, the corrosion rate for the copper immersed for 24 h decreases approximately one order of magnitude, indicating that corrosion processes are suppressed. However, after immersion for 720 h, the corrosion current density increases approximately two orders of magnitude, showing an enhanced corrosion rate. The variation of R_p is also consistent with the above analysis.

3.2.2 Electrochemical impedance spectroscopy

Typical Nyquist and Bode plots for the corrosion of copper in the electrolyte containing ethylene carbonate (EC) and methyl ethyl carbonate (EMC) and dimethyl carbonate (DMC) after immersion for varying lengths of time are shown in Figure 3. All spectroscopy plots consist of two depressed capacitive loops. The capacitive loop at high frequency corresponds to the impedance response of the corrosion product layer on the copper, while the loop at low frequency was related to the responses from the electrochemical reaction occurring at the electrolyte/copper interface. The capacitive loops expand significantly from 3 h to 24 h indicating the formation of a protective film on the surface of copper, which is duly supported by the increase in the phase angle in the low and middle frequency regions as shown in Figure 3b. However, the capacitive loop contracts from 48 h to 150 h. Correspondingly, the contraction is accompanied by the gradual depression of the phase angle, which suggests the dissolution of the corrosion product. With the extension up to 720 h, the impedance decreases in fluctuation.

The impedance behavior of the copper is fitted using the equivalent electrical circuit (EEC) shown in Figure 4, where R_s represents the electrolyte resistance, R_f and Q_f represent the resistance and capacitance of the corrosion product layer that forms on the copper surface, and R_t and Q_{dl} represent the charge transfer resistance and the double layer capacitance. The simulated impedance data are in good agreement with the experimental data shown in Figure 3, where symbols represent the experimental data and the lines represent the fitting. In this EEC, a constant phase element, CPE (Q), replaces a capacitor (C) to take into account the surface reactivity, surface heterogeneity, roughness, electrode porosity and current and potential distributions associated with the electrode geometry. [16]

The impedance of the CPE can be expressed as Equation 2: [17]

$$Z_{CPE} = \frac{1}{Y_0} (j\omega)^{-n} \quad (2)$$

where Y_0 represents the admittance magnitude of the CPE and n is the exponential term. Pure capacitance behavior of the corrosion system is represented by $n = 1$. However, the value of n usually varies from 0 to 1 for a practical system. A small value of n is often attributed to a rough electrode surface. [18] The maximum error is less than 2.5% in $|z|$ and less than 4% for the angle of all fitted impedance spectra. Figure 5 shows a representative error plot for the copper.

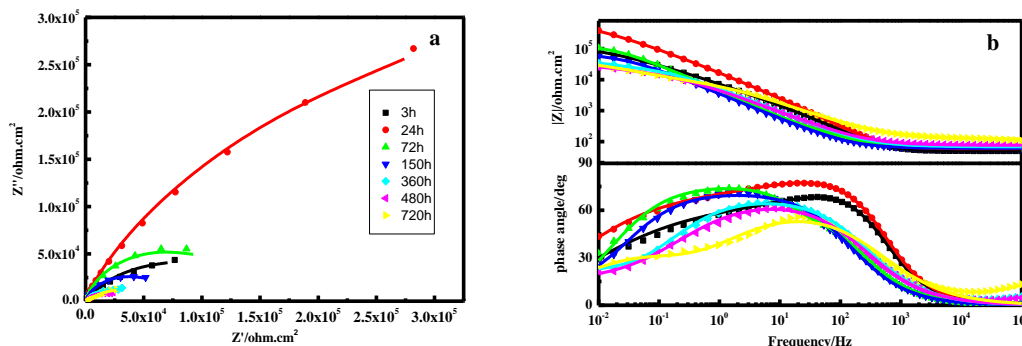


Figure 3. (a) Nyquist and (b) Bode plots for the copper in electrolyte at room temperature with prolonged immersion times (symbols: experimental data; line: fitted data)

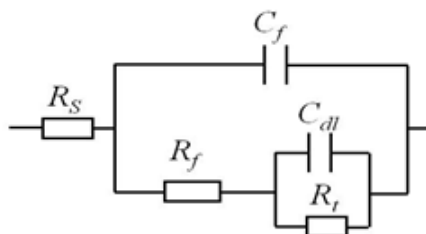


Figure 4. Equivalent circuit for fitting the impedance data of copper in the electrolyte

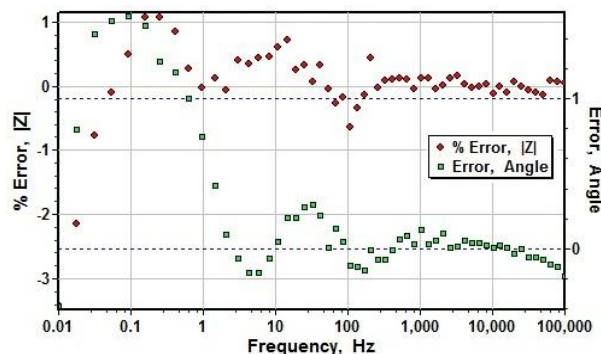


Figure 5. Error plots for calculated values of $|z|$ and the phase angle of copper immersed for 24h in the electrolyte.

Figure 6 presents the fitted R_f and R_t of copper in the electrolyte. R_f increases after immersion for 24 h and then decreases upon further exposure to 96 h. Similar fluctuations exist up to 420 h and then a decrease until to 720 h. However, R_t increases significantly after immersion for 24h. Subsequently, R_t declines suddenly and remain nearly stable from 72 h to 720 h of immersion. R_f represents the resistance of the oxide layer or corrosion product layer on the copper surface, while R_t is related to the surface of metal/electrolyte interface in electrochemical processes. The increase of R_f and

R_t at the initial stage (i.e. 3 h -24 h) can be attributed to the formation of a protective film on the copper that inhibits the attack of aggressive species. After immersion for 420 h, R_f decreases significantly, indicating that a porous corrosion product layer forms. The results are consistent with those from the potentiodynamic curves, as shown in Figure 2.

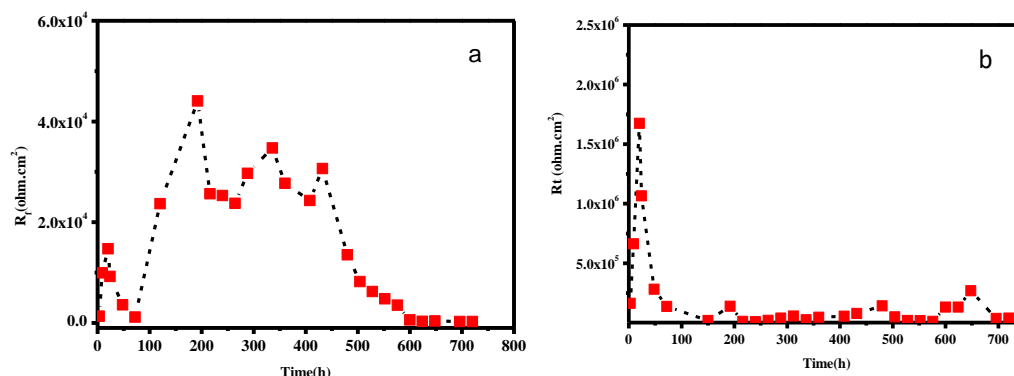


Figure 6. The fitted (a) R_f and (b) R_t versus time for the corrosion of copper in the electrolyte

3.3 Proposed corrosion mechanism of copper in the electrolyte

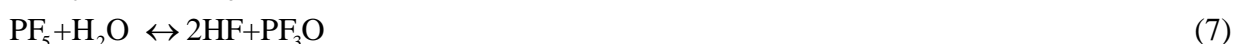
The decrease in impedance confirms that the copper is subject to corrosion damage in the electrolyte of lithium-ion batteries. It has been accepted that the trace amount of water in the electrolyte causes the corrosion of current collectors of lithium-ions batteries. [19] Copper could be oxidized by water with the formation of copper oxide, meanwhile, it acts as anodic reaction of electrochemical corrosion. [20] The reaction is as follows:



The oxygen reduction as a cathodic reaction could be negligible in such a closed system. However, EC and DMC in the electrolyte could be reduced to compounds that absorb on the surface of copper: [21, 22]



Meanwhile, LiPF_6 could decompose spontaneously and react with the trace amount of water in the electrolyte, producing HF and PF_3O . [23] HF in the trace amount of water results in a significant decrease in pH. Copper can hardly be corroded in a deoxygenated acid solution. [24-25] Nevertheless, copper oxide would dissolve in the solution containing HF. The reactions are expressed as follows:



Therefore, the increasing impedance of copper after exposure to the electrolyte for 24 h (as shown in Figure 3) correlates with the consumption of water and the formation of copper oxide. In addition, it is acknowledged that solid electrolyte interphase (SEI) layer could form on the metal because of the electrolyte decomposition during storage. [26] This also contributes to suppressing the anodic dissolution of copper. Subsequently, F^- stemming from the decomposition of $LiPF_6$ absorbs on the copper oxide and results in its dissolution, which suggests a decrease in the corrosion resistance. As mentioned above, the trace amount of water promotes the formation of CuO_x and HF, while F^- would attack CuO_x accompanied by the generation of water. Therefore, R_f fluctuates during immersion up to 420 h in the electrolyte..

Theoretically, electrochemical corrosion is a process that initially forms oxide films and subsequently destroys the films. [27] As the reaction in Eq (8) occurs, galvanic coupling is then established between the sites of attacked copper oxide and the intact sites, which form small anodes where metal dissolution occurs, and the remainder of the surface where the cathodic reaction occurs. Namely, pitting corrosion induced by F^- occurs on the surface of copper. Moreover, the H^+ produced by reaction (3) decreases the pH locally, resulting in an activation solution of the copper oxide. With an increase in the concentration of metal ions and accumulation of positive charge, a strong electric field is formed and attracts PF_6^- or decomposed F^- into the inside of the holes. Under the combined effect of the H^+ and F^- , the pitting holes continues to dissolve by self-catalyzed effect. [28] Therefore, the holes develop with extended exposure time. The elements P and F detected in the pitting holes, as shown in Figure 1 b, also confirm the above analysis. With the extension of the immersion time in the electrolyte, the various organic and inorganic compounds produced by the spontaneous decomposition or electrochemical reduction of the electrolyte (EM and DMC) deposit on the surface of copper with the formation of a porous corrosion product layer. [12] Thus, R_f decreases after immersion in the electrolyte for 420 h. In addition, additional C and O can be observed compared with P and F in the pitting holes on the copper after corrosion for 720 h, as shown in Figure 1c.

Copper usually suffers pitting corrosion after exposure to different conditions. In many cases, copper pitting corrosion proceeds via coupling between the oxidation of copper at small anode sites and reduction of oxidants such as oxygen on large surface areas. [29] In this work, the copper current collector tends to suffer pitting corrosion in the non-aqueous electrolyte, in which the electrochemical reduction of an organic electrolyte as the cathodic reaction couples with the dissolution of copper. In fact, there exists a kind of complex reaction in the electrolyte during long-term storage. It should be noted that this study concerns the corrosion behavior of copper in the organic electrolyte of lithium-ion batteries based on electrochemical principles, and it provides certain information about the corrosion behavior of copper in the electrolyte during long-term immersion. Our research further includes the variation in the electrolyte with time and its effects on the microstructural evolution of copper.

4. CONCLUSIONS

Electrochemical approaches were used to evaluate the corrosion behavior of a copper current collector in the electrolyte of lithium-ions batteries with long-term immersion. Compared with the

specimens immersed in the electrolyte for 3 h, the corrosion current density decreases by one order of magnitude for the specimens exposed to the electrolyte for 24 h, while it increases by more than one order of magnitude for 720 h of immersion. Similarly, R_f and R_t increase after immersion in the electrolyte for 24 h, which correlates with the oxidation of copper by the trace amount of water in the electrolyte and the formation of a solid electrolyte interphase (SEI) layer. Then, in the case of R_f , a fluctuation exists until 420 h of exposure to the electrolyte, which is due to the formation and dissolution of oxygenated compounds on the copper surface. HF stemming from the decomposition of LiPF_6 in the electrolyte causes the successive pitting corrosion on the surface of copper because of a self-catalyzed effect.

ACKNOWLEDGMENTS:

This work was supported by the National Natural Science Foundation of China (No.51471036), Key Project of Hunan Province Science and Technology Department (No.2014GK2010), and funded by Changsha University of Science & Technology (No.CX2017SS15) and Hunan Province 2011 Collaborative Innovation Center of Clean Energy and Smart Grid.

References

1. T. Horiba, *P. IEEE.*, 102(6) (2014) 939-950.
2. A. Yoshino, *Angew. Chem.*, 51(24) (2012) 5798.
3. C. Lan, J. Xu, Y. Qiao and Y. Ma, *Appl. Therm. Eng.*, 101 (2016) 284-292.
4. M. Jeong, M. Lee, J. Cho and S. Lee, *Adv. Energy Mater.*, 5(13) (2015).
5. M. Jing, M. Zhou, G. Li, Z. Chen, W. Xu, X. Chen and Z. Hou, *ACS Appl. Mater. & Inter.*, 9(11) (2017) 9662.
6. C.H. Tan, G.W. Qi, Y.P. Li and S.Y. Zhang, *Int. J. Electrochem. Sci.*, 8(2) (2013) 1966-1975.
7. Z. Wu, R.R. Huang, H. Yu, Y.C. Xie, X.Y. Lv, J. Su, Y.F. Long and Y.X. Wen, *Materials*, 10(2) (2017) 134.
8. X. Zhang, B. Winget, M. Doeff, J.W. Evans and T.M. Devine, *J. Electrochem. Soc.*, 152 (11) (2005) 1310-7.
9. T.C. Hyams, J. Go and T.M. Devine, *J. Electrochem. Soc.*, 154 (8) (2007).
10. E. Kramer, S. Passerini and M. Winter, *Ecs. Electrochem. Lett.*, 1(5) (2012) C9-C11.
11. B. Streipert, S. Röser, J. Kasnatscheew, P. Janßen, X. Cao and R. Wagner, *J. Electrochem. Soc.*, 164(7) (2017) A1474-A147
12. J. Shu, M. Shui, F. Huang, D. Xu, Y. Ren, L. Hou, J. Cui and J. Xu, *Electrochim. Acta.*, 56(8) (2011) 3006-3014.
13. C. Peng, L. Yang, S. Fang, J. Wang, Z. Zhang, K. Tachibana, Y. Yang and S. Zhao, *J. Appl. Electrochem.*, 40(3) (2010) 653-662.
14. M. Zhao, S. Kariuki, H.D. Dewald, F.R. Lemke, R.J. Staniewicz, E.J. Plichta and R.A. Marsh, *J. Electrochem. Soc.*, 147(8) (2000) 2874-2879.
15. E. Hayfronbenjamin, *Biochem. J.*, 234(3) (2013) 507-14.
16. M.E. Orazem, I. Frateur, B. Tribollet and M. Musiani, *J. Electrochem. Soc.*, 160(6) (2013) C215-C225.
17. Y.J. Ren, J. Chen, C.L. Zeng, C. Li and J.J. He, *Int. J. Hydrogen Energ.*, 41(20) (2016) 8542-8549.
18. X. Wu, H. Ma, S. Chen, Z. Xu and A. Sui, *J. Electrochem. Soc.*, 146(5) (1999) 1847-1853.
19. D. Aurbach, I. Weissman, A. Zaban and P. Dan, *Electrochim. Acta.*, 45(7) (1999) 1135-1140.
20. T.J. Chem, A. Naseer and A.Y. Khan, *Turk. J. Chem.*, 34(5) (2014) 815-824.
21. N. Gang, R.E. White and B.N. Popov, *Electrochim. Acta.*, 51(10) (2006) 2012-2022.

22. G. Ning, B. Haran and B.N. Popov, *J. Power Sources*, 117(1–2) (2003) 160-169.
23. S.T. Myung, Y. Sasaki, S. Sakurada, Y. Sunb and H. Yashiroa, *Electrochim. Acta.*, 55(1) (2009) 288-297.
24. A.M. Eldesoky, M.A. Diab, A.A. El-Bindary and A.H. Seyam, *J. Mater. Environ. Sci.*, 6(8) (2015) 2148-2165.
25. A.S. Fouda, A.M. Eldesoky, A.Z. El-Sonbati and S.F. Salam, *Int. J. Electrochem. Sci.*, 9(4) (2014) 1867-1891.
26. N. N. Sinha, J. C. Burns and J. R. Dahn, *J. Electrochem. Soc.*, 160(4) (2013) A709-A714.
27. J.Z. Lu, B. Han, C.Y. Cui, C.J. Li and K.Y. Luo, *Opt. Laser Technol.*, 88 (2017) 250-262.
28. T.J. Yang, G.M Li, S. Chen, W.S. Chang and X.Q. Chen, *Corros. & Prot.*, 07 (2010).
29. G. Subramanian, S. Palraj and S. Palanichamy, *J. Mari. Sci. Appl.*, 13(2) (2014) 230-236.

© 2017 The Authors. Published by ESG (www.electrochemsci.org). This article is an open access article distributed under the terms and conditions of the Creative Commons Attribution license (<http://creativecommons.org/licenses/by/4.0/>).